

Published in final edited form as:

*Nat Immunol.* 2009 June ; 10(6): 603–609. doi:10.1038/ni.1736.

## A protective function for interleukin 17A in T cell-mediated intestinal inflammation

William O'Connor Jr<sup>1</sup>, Masahito Kamanaka<sup>1</sup>, Carmen J Booth<sup>2</sup>, Terrence Town<sup>1,6</sup>, Susumu Nakae<sup>3</sup>, Yoichiro Iwakura<sup>3</sup>, Jay K Kolls<sup>4</sup>, and Richard A Flavell<sup>1,5</sup>

<sup>1</sup>Department of Immunobiology, Yale University School of Medicine, New Haven, Connecticut, USA.

<sup>2</sup>Section of Comparative Medicine, Yale University School of Medicine, New Haven, Connecticut, USA.

<sup>3</sup>Center for Experimental Medicine, Institute of Medical Science, University of Tokyo, Tokyo, Japan.

<sup>4</sup>Children's Hospital of Pittsburgh, Pittsburgh, Pennsylvania, USA.

<sup>5</sup>Howard Hughes Medical Institute, Yale University, New Haven, Connecticut, USA.

### Abstract

Interleukin 23 (IL-23) and IL-17 have been linked to the pathogenesis of several chronic inflammatory disorders, including inflammatory bowel disease. Yet as an important function for IL-23 is emerging, the function of IL-17 in inflammatory bowel disease remains unclear. Here we demonstrate IL-17A-mediated protection in the CD45RB<sup>hi</sup> transfer model of colitis. An accelerated wasting disease elicited by T cells deficient in IL-17A correlated with higher expression of genes encoding T helper type 1-type cytokines in colon tissue. IL-17A also modulated T helper type 1 polarization *in vitro*. Furthermore, T cells deficient in the IL-17 receptor elicited an accelerated, aggressive wasting disease relative to that elicited by wild-type T cells in recipient mice. Our data demonstrate a protective function for IL-17 and identify T cells as not only the source but also a target of IL-17 *in vivo*.

The interleukin 23 (IL-23)–IL-17 axis is emerging as a critical regulatory system that bridges the innate and adaptive arms of the immune system. The IL-12 cytokine family member IL-23 is secreted by ‘professional’ antigen-presenting cells during inflammatory responses to pathogenic as well as nonpathogenic stimuli<sup>1</sup>. IL-23 elicits myriad effector molecules, most notably IL-17A, IL-17F and tumor necrosis factor, as well as others, depending on the responder cell<sup>2,3</sup>. Among the cell types known to respond to IL-23 are antigen-experienced CD4<sup>+</sup> T lymphocytes, which express surface IL-23 receptor (IL-23R) complexes and rapidly produce proinflammatory cytokines, including interferon- $\gamma$  (IFN- $\gamma$ ) and IL-17, within hours of IL-23 stimulation<sup>2,4</sup> (W.O., unpublished observations). Of particular interest is IL-23-mediated production of IL-17, which has been reported to be important in the pathogenesis of

© 2009 Nature America, Inc. All rights reserved.

Correspondence should be addressed to R.A.F. (E-mail: richard.flavell@yale.edu).

<sup>6</sup>Present address: Department of Neurosurgery, Biomedical Sciences and Department of Medicine, Maxine Dunitz Neurosurgical Institute Cedars-Sinai Medical Center, Los Angeles, California, USA.

#### AUTHOR CONTRIBUTIONS

W.O. and R.A.F. designed the study and wrote the manuscript; M.K. provided flow cytometry data, advice and technical guidance; W.O. did all other *in vitro* and *in vivo* experimental work; C.J.B. did histopathological scoring analyses; T.T. provided assistance with statistical analyses; Y.I. and S.N. provided *Il17a*<sup>−/−</sup> mice; and J.K.K. provided the *Il17ra*<sup>−/−</sup> mice.

Supplementary information is available on the Nature Immunology website.

Reprints and permissions information is available online at <http://npg.nature.com/reprintsandpermissions/>

several inflammatory disorders, including the initiation and/or progression of experimental autoimmune encephalomyelitis, a mouse model of human multiple sclerosis<sup>5,6</sup>. IL-17 is thought to exert proinflammatory effects mainly by eliciting the production of CXC chemokines and other chemoattractants from both endothelial and epithelial cells, which nearly ubiquitously express the IL-17 receptor (IL-17R)<sup>7,8</sup>. Neutrophils and other cells of the immune system are subsequently recruited, thereby amplifying the inflammatory episode<sup>9,10</sup>.

The IL-23-IL-17 system has also been linked to inflammatory bowel disease (IBD). Genome-wide analyses have identified several uncommon *Il23r* variants inversely correlated with susceptibility to IBD<sup>11,12</sup>. In addition, there is higher expression of IFN- $\gamma$  and IL-17 in the intestinal mucosa of patients with Crohn's disease<sup>13,14</sup>. In mouse colitis studies using either adoptive transfer of CD45RB<sup>hi</sup> T cells or infection with helicobacter to induce IBD, investigators have documented expression of IL-23, IL-17 and IFN- $\gamma$  in the inflamed colon tissue<sup>15-17</sup>. In these studies, the expression of IFN- $\gamma$  and IL-17 is dependent on recipient mouse-derived IL-23, and disease development in recipient mice is nearly completely dependent on the presence of IL-23, which indicates IL-23 is a critical factor in the initiation of mouse IBD. This has led to speculation that IFN- $\gamma$  and IL-17 may act in synergy to initiate colon inflammation. However, as other studies have shown that neutralization of IFN- $\gamma$  nearly completely abrogates T cell-mediated intestinal damage and wasting disease<sup>18</sup>, and the adoptive transfer of IFN- $\gamma$  deficient cells also fails to induce disease in recipient mice<sup>19</sup>, IFN- $\gamma$  has been shown to be critical for IBD in these models, whereas the function of IL-17 in these experimental systems has remained unclear. Indeed, the function of IL-17A in intestinal inflammation has thus far remained controversial. An inflammatory function for IL-17 in trinitrobenzenesulfonic acid-induced colitis has been described<sup>20</sup>, yet another report has suggested IL-17 might offer protection in the dextran sodium sulfate-induced colitis model<sup>21</sup>. Notably, chemically induced intestinal damage in those models is T cell independent<sup>22</sup> and more accurately reflects the chronic stage of disease after compromise of the epithelial barrier, rather than early disease-initiating events.

Here we show that IL-17A mediates a protective effect on T cell-driven intestinal inflammation *in vivo*. Using a well-established mouse transfer model of colitis, we found that relative to wild-type populations, *Il17a*<sup>-/-</sup> CD45RB<sup>hi</sup> cells induced a more aggressive wasting disease when transferred into recipient mice deficient in recombination-activating gene 1 (*Rag1*<sup>-/-</sup>). Cohorts that developed accelerated IBD had higher expression of IFN- $\gamma$  and osteopontin mRNA in resected colon tissue at the onset of intestinal tissue damage, as well as weight loss, which provides evidence that classical T helper type 1 (T<sub>H</sub>1)-associated cytokines, not IL-17, probably drive disease initiation. Consistent with those observations, *Il17a*<sup>-/-</sup> CD45RB<sup>hi</sup> cells polarized to T<sub>H</sub>1 effectors *in vitro* had higher expression of IFN- $\gamma$  and the T<sub>H</sub>1 'master regulator' T-bet, and recombinant IL-17 inhibited the expression of these factors in developing wild-type T<sub>H</sub>1 cells. Furthermore, CD45RB<sup>hi</sup> cells deficient in IL-17R (*Il17ra*<sup>-/-</sup>) also elicited an accelerated aggressive wasting disease relative to that in recipients of wild-type T cells in the transfer model. Our findings demonstrate that IL-17A provides protection in this model of T cell-mediated wasting disease and that T cells are responsive to IL-17A *in vivo*, and they identify T cells as both the source and the relevant target of IL-17 in this experimental system. Our observations collectively have implications for strategies that aim to modulate the IL-23-IL-17 immune axis for clinical benefit.

## RESULTS

### IL-17A modulates T cell-driven colitis

To directly assess the function of IL-17A in T cell-mediated colitis, we adoptively transferred purified CD45RB<sup>hi</sup> CD25<sup>-</sup>CD4<sup>+</sup> T cells from *Il17a*<sup>-/-</sup> mice or wild-type mice into *Rag1*<sup>-/-</sup> recipients and then monitored wasting disease in the recipients. Wild-type CD4<sup>+</sup> CD45RB<sup>hi</sup>

T cells predictably induced wasting disease 5–7 weeks after transfer (Fig. 1a). Cohorts that received *Il17a*<sup>-/-</sup> T cells however, developed an overly aggressive inflammatory disease relative to that of recipients of wild-type cells, as shown by their accelerated decrease in body mass (Fig. 1a,b). There was divergence in body-mass curves by 4 weeks after adoptive transfer, and repeated-measures analysis of variance (ANOVA) showed significant main effects of time ( $P < 0.001$ ) and experimental group ( $P < 0.05$ ) and a time-group interaction ( $P < 0.05$ ) in the composite data analysis of three independent experiments (Fig. 1b). There was a significant difference at 4.0–4.5 weeks after adoptive transfer of CD4<sup>+</sup> CD45RB<sup>hi</sup> T cells (post-hoc *t*-test). Recipients of *Il17a*<sup>-/-</sup> CD4<sup>+</sup> CD45RB<sup>hi</sup> T cells reached the humane weight-loss limit more rapidly (80% of original mass, which required that mice be killed), in some cases as many as 2 weeks earlier than controls (Fig. 1 and data not shown). Indeed, by 6 weeks after transfer, the 80% mass-loss target had been reached by over 40% of *Rag1*<sup>-/-</sup> recipients of *Il17a*<sup>-/-</sup> CD45RB<sup>hi</sup> cells (Fig. 1a,b and data not shown). Disease incidence was 94.3% and 92.1% for recipients of wild-type cells and *Il17a*<sup>-/-</sup> cells, respectively. Thus, CD45RB<sup>hi</sup> cells unable to produce IL-17A induced an aggressive wasting disease *in vivo*, which demonstrates IL-17A is not critical in the initiation of T cell-induced colitis in this model. Moreover, it seems that in this model system, IL-17A delayed the kinetics of disease onset, which emphasizes a previously unappreciated protective function for IL-17A in intestinal inflammation. Notably, the cotransfer of IL-17A-deficient regulatory T cells completely inhibited colitis in this model (Supplementary Fig. 1 online), which suggests that although IL-17A may be protective, regulatory T cell-mediated suppression is IL-17A independent.

### More T<sub>H</sub>1-associated inflammation in recipients of *Il17a*<sup>-/-</sup> T cells

To gain insight into the mechanisms driving the accelerated colitis in the absence of IL-17A, we examined recipients of *Il17a*<sup>-/-</sup> CD45RB<sup>hi</sup> T cells at 2 weeks and 4 weeks after adoptive transfer. Overall body mass was maintained or slightly higher in the first 2 weeks after transfer in all groups (Fig. 1b and data not shown). However, greater organ thickness, cellular infiltration and edema and disrupted tissue architecture were already observable in ascending and descending colon tissue from mice at autopsy 2 weeks after transfer (Fig. 1c,d). In the colons of recipients of wild-type cells, we found normal mucosa, minimal submucosa and unremarkable muscularis externa (Fig. 1d, i). By day 14, colons from mice given *Il17a*<sup>-/-</sup> cells had an overall thinner wall, with mild to moderate submucosal edema (Fig. 1d, ii, and e), in contrast to mice given wild-type cells, which had a much thicker colon (Fig. 1d, iii, and e), mainly due to moderately to considerably greater thickness at the level of the submucosa and muscularis (Supplementary Fig. 2 online). The overall severity of cellular infiltration, generally assigned a score as 'inflammation', was equivalent in the groups (Fig. 1e); however, several recipients of *Il17a*<sup>-/-</sup> cells had severe ulceration with considerable loss of mucosal epithelial cells (Fig. 1d, iv, v, and e). The transition to ulcerated epithelium was notable (Fig. 1d, v). By day 28, colons from mice that received wild-type cells showed similar inflammation without the severe mucosal epithelial ulceration (Fig. 1d, vi,vii). We assigned scores to histopathological criteria semiquantitatively (Fig. 1e). In general, the severity of ulceration, inflammation, edema and observable tissue damage was greater in individual mice with the greatest weight loss in the group, concomitant with meaningful differences in body mass at day 28. We concluded that the greater severity of wasting disease mediated by *Il17a*<sup>-/-</sup> CD45RB<sup>hi</sup> T cells was probably not due to differences in cellular infiltration of the colon (Fig. 1e) but may instead have been due to relative changes in effector T cell function.

Next we assessed the expression of T<sub>H</sub>1 cell-associated cytokines traditionally associated with T cell-mediated IBD. Quantitative RT-PCR showed that the expression of mRNA transcripts encoding T<sub>H</sub>1-associated factors was higher in colon tissue from recipients of *Il17a*<sup>-/-</sup> cells than in that of recipients of wild-type cells (Fig. 1f). Notably, *Ifng* expression was threefold higher in recipients of *Il17a*<sup>-/-</sup> T cells. *Tnf* expression was not similarly higher (Fig. 1f). In

addition, expression of *Spp1* mRNA, which encodes osteopontin, a cytokine that amplifies T<sub>H</sub>1-type responses through the induction of IL-12 and other mechanisms<sup>23,24</sup>, was ninefold higher in recipients of *Il17a*<sup>-/-</sup> cells (Fig. 1f). *Il6* expression trended upward in the group of recipients of *Il17a*<sup>-/-</sup> cells, but this result was not statistically significant. We found no difference in *Tnf* expression in recipients of *Il17a*<sup>-/-</sup> cells or wild-type cells (Fig. 1f). We detected these differences in cytokine mRNA expression at 28 d after cell transfer but not at 14 d after cell transfer or in samples obtained at the disease endpoint (typically 8–10 weeks), when epithelial damage and cellular infiltration was extensive (data not shown). Additionally, expression of *Il17a* and *Il17f* mRNA was nearly undetectable in recipient colon tissue obtained at 28 days after transfer (Supplementary Fig. 3 online), which suggests that neither IL-17A nor IL-17F contributes much to the disease in this model.

Colon tissue from recipients of *Il17a*<sup>-/-</sup> T cells had higher expression of *Il22* mRNA at day 28 than did that of recipients of wild-type cells; however, studies with transfers of *Il17a*<sup>-/-</sup>*Il22*<sup>-/-</sup> CD45RB<sup>hi</sup> cells showed that increased T cell-derived IL-22 was not responsible for the accelerated wasting disease noted in the absence of T cell-derived IL-17 (Supplementary Fig. 4 online). These results demonstrate that cohorts that received *Il17a*<sup>-/-</sup> CD45RB<sup>hi</sup> T cells, which developed an accelerated wasting disease, had higher expression of T<sub>H</sub>1-associated cytokines in inflamed colon tissue. Larger amounts of T<sub>H</sub>1-associated cytokines may have resulted in the observed lower overall body mass. These data therefore suggest that the accelerated colitis in recipients of *Il17a*<sup>-/-</sup> T cells may have been due at least in part to the acceleration of a T<sub>H</sub>1 differentiation program *in vivo*.

### IL-17A signaling in T cells suppresses T<sub>H</sub>1 differentiation

On the basis of our *in vivo* observations, we hypothesized that T cells may be directly responsive to IL-17A. The IL-17 receptor (IL-17R) was nearly undetectable on naive CD4<sup>+</sup> T cells (Fig. 2a). In contrast, IL-17R was upregulated at late stages during the T<sub>H</sub>1 differentiation program, with moderate amounts of cell surface IL-17R detectable by day 4 (Fig. 2a). We confirmed our flow cytometry results by immunoprecipitation and immunoblot analysis, which showed that total cellular IL-17R protein quantities were low in naive T cells (Fig. 2b) but were modestly induced during T<sub>H</sub>1 development *in vitro* (Fig. 2b). The IL-17R can be visualized as a protein of approximately 120 kilodaltons, a value much larger than the predicted molecular weight based on amino acid analysis (98 kilodaltons). *In silico* analysis of the protein sequence of IL-17R showed that extensive N-glycosylation was predicted with high probability (five asparagine residues predicted by the NetNGlyc 1.0 Server (Technical University of Denmark); seven predicted sites reported in the UniProtKB/Swiss-Prot entry). To determine if glycosylation accounted for the shift in molecular weight, we deglycosylated the immunoprecipitated IL-17R with peptide N-glycosidase F and found that after treatment, the doublet migrating at approximately 120 kilodaltons resolved to a single band visualized by immunoblot at the predicted 98 kilodaltons (Fig. 2b).

We next sought to determine whether purified IL-17 could exert appreciable effects on the development of wild-type T<sub>H</sub>1 cells *in vitro*. We cultured sorted naive CD45RB<sup>hi</sup> CD4<sup>+</sup> T cells for 4 d in T<sub>H</sub>1-polarizing conditions in the presence or absence of recombinant IL-17. Treatment with IL-17 resulted in much lower expression of the T<sub>H</sub>1-associated mRNA transcripts *Ifng*, *Spp1* and *Il12rb2* (Fig. 2c), which showed that recombinant IL-17 exerted broadly suppressive effects on the T<sub>H</sub>1 developmental program. Transcripts encoding SOCS3, a known inhibitor of IL-17 production<sup>25</sup>, were also lower in abundance after treatment with recombinant IL-17, whereas IL-17 had no effect on SOCS1 mRNA (Fig. 2c). IL-17 also led to a 78% lower abundance of phosphorylated STAT1 (Fig. 2d). The addition of neutralizing antibody to IL-17 completely reversed the IL-17-mediated suppression of phosphorylated STAT-1 (Fig. 2d). Expression of T-bet, a transcription factor essential for T<sub>H</sub>1 differentiation,

was also much lower in IL-17-containing cultures (Fig. 2d). As with STAT1, the effect on T-bet was reversed by IL-17-neutralizing antibody (Fig. 2d). Recombinant IL-17 did not substantially affect the expression of genes encoding IL-9, granulocyte-macrophage colony-stimulating factor, the chemokine CCL3, IL-1 $\beta$  or the chemokine CXCL1 in developing T<sub>H</sub>1 cells or induce the expression of T<sub>H</sub>17-specific genes in developing T<sub>H</sub>17 cells (Supplementary Figs. 5 and 6 online and data not shown).

To determine if IL-17 affected expression of *Tbx21*, which encodes T-bet, we again cultured sorted naive CD45RB<sup>hi</sup> CD4<sup>+</sup> T cells in T<sub>H</sub>1-polarizing conditions in the presence or absence of recombinant IL-17. Recombinant IL-17 potently inhibited *Tbx21* expression as early as 48 h after stimulation (Fig. 3a). By day 4 of *in vitro* polarization, *Tbx21* expression in IL-17-containing T<sub>H</sub>1 cultures was less than 10% of that in cultures without recombinant IL-17 (Fig. 3a). Lower *Tbx21* expression preceded the diminished T-bet protein; we first noted the latter after 4 d of culture (Fig. 3b). The diminished T-bet was not due to lower rates of cellular proliferation, as assessed by incorporation of [<sup>3</sup>H]thymidine (Fig. 3c). Notably, the addition of IL-17 to wild-type T<sub>H</sub>1 cultures on day 4 did not lower the already robust T-bet expression (data not shown). Therefore, whereas IL-17 does not seem to extinguish T-bet expression in mature T<sub>H</sub>1 cells, our studies suggest IL-17 can inhibit the upregulation of T-bet that normally occurs during early stages of the T<sub>H</sub>1 differentiation program. Consistent with involvement of IL-17A in repressing T<sub>H</sub>1 development, purified *Il17a*<sup>-/-</sup> CD45RB<sup>hi</sup> CD4<sup>+</sup> T cells cultured in standard T<sub>H</sub>1-type conditions had higher expression of *Tbx21* (Fig. 3d). After restimulation, *Il17a*<sup>-/-</sup> T<sub>H</sub>1 cells also secreted more IFN- $\gamma$  protein (Fig. 3e). However, the presence or absence of IL-17A did not substantially affect cellular proliferation (Fig. 3f). These data, which show that IL-17 antagonizes the T<sub>H</sub>1 differentiation program *in vitro*, further support our *in vivo* data demonstrating a more rapid T<sub>H</sub>1-associated disease course in the absence of IL-17.

### IL-17R-deficient T cells elicit an aggressive wasting disease

On the basis of our findings demonstrating that T cells can respond to IL-17, we hypothesized that the accelerated inflammation noted *in vivo* may have been due to T cell–intrinsic IL-17 acting in an autocrine way. To test our hypothesis, we did additional colitis experiments with IL-17R-deficient donor T cells. Like *Il17a*<sup>-/-</sup> cells, the *Il17ra*<sup>-/-</sup> CD45RB<sup>hi</sup> CD4<sup>+</sup> T cells also elicited an accelerated wasting disease in *Rag1*<sup>-/-</sup> recipients (Fig. 4a). Accelerated weight loss was first evident at day 35, and at days 42 and 49, differences in body mass were even more apparent (Fig. 4a, Table 1 and Supplementary Fig. 7 online). Histologically, scores for all criteria were the same for recipients of *Il17a*<sup>-/-</sup> or *Il17ra*<sup>-/-</sup> cells, with a consistent loss of crypts in the mucosa and inflammatory infiltrates both in the mucosa and submucosa readily observable by day 28 (Fig. 4b,c). These data collectively demonstrate that in this experimental system, the transferred CD4<sup>+</sup> CD45RB<sup>hi</sup> T cells were both the source and the relevant target of IL-17 *in vivo*.

## DISCUSSION

Higher IL-17 expression in the gut during intestinal inflammation, found in mouse models and in human disease, led us to begin investigating how IL-17 contributes, if at all, to the initiation and pathogenesis of IBD. Our results have shown that in the CD45RB<sup>hi</sup> transfer model of colitis, an accelerated wasting disease resulted when adoptively transferred T cells were unable to produce IL-17 or failed to express IL-17R. Although the function of IL-17 in the initiation and pathogenesis of IBD has been controversial, our findings demonstrate a protective function for IL-17 in this experimental system. Notably, our results are in agreement with a report suggesting IL-17 could serve a protective function in the gut, albeit in a T cell-independent model of wasting disease<sup>21</sup>. Those findings were subsequently supported by studies done elsewhere<sup>26</sup>.

Several studies have identified IL-23, one of the most potent inducers of IL-17, as being critical for IBD in mouse models assessing intestinal inflammation in the absence of IL-10 or in response to helicobacter infection<sup>15,16</sup>. Investigators have explored the relative importance of the contributions of IL-23 and IL-12 in intestinal inflammation with genetically deficient T cells in adoptive-transfer studies and measuring tissue infiltration and inflammation by assigning scores for histological criteria. IL-23 is inarguably critical for tissue inflammation in those models and furthermore, although the results are not statistically significant, daily administration of antibody to IL-17 (anti-IL-17) during the disease course does seem to provide some benefit, diminishing intestinal inflammation scores<sup>16</sup>. These results are not unexpected, given that the proinflammatory properties of IL-17 and of IL-17-producing cells are well established. Indeed, it remains possible that IL-23-mediated IL-17 contributes, perhaps in a nonessential way, to the recruitment of cells of the immune system to the inflamed colon during intestinal inflammation. It is important to note that in our studies, the extent of cellular infiltration did not correlate with the wasting aspect of the disease. In recipients of wild-type T cells, *Il17a*<sup>-/-</sup> T cells or *Il17ra*<sup>-/-</sup> T cells, we noted extensive cellular infiltration, organ thickness, loss of crypts, loss of glands and edema; the greatest differences we noted were differences in recipient mouse weight loss during the ensuing wasting disease, after accumulation of cellular infiltrate in the recipient colon tissue. We conclude from our observations that infiltration of cells of the immune system is probably only one of several important components that direct the pathogenesis seen in this wasting disease and that perhaps there might be considerable differences in the functional abilities of the infiltrating cells. Our results showing higher expression of genes encoding T<sub>H</sub>1-type cytokines in colon tissue of recipients of *Il17a*<sup>-/-</sup> T cells suggest this may be the case. At day 28 after adoptive transfer, we detected elevated expression of the genes encoding IFN- $\gamma$  and osteopontin in the inflamed colons of recipients of *Il17a*<sup>-/-</sup> T cells, concomitant with notable epithelial cell death and, in some cases, exposure of entire regions of the lamina propria to the gut lumen, as noted histologically.

One possibility is that IL-23-induced IL-17 is one of many factors that does contribute, in certain circumstances (such as in the absence of IL-10), to intestinal inflammation, whereas other IL-23-induced factors are responsible for tissue damage, in an IL-17-independent way. The idea that IL-23 uses 'downstream' effectors other than IL-17 in mediating inflammatory events is consistent with our findings and with published results of intestinal inflammation studies<sup>15,16</sup>. In addition, IL-23 has been shown to specifically use IL-22 to mediate dermal acanthosis<sup>27</sup>. Notably, in our studies, *Il22* mRNA was substantially upregulated in colon tissue in recipients of *Il17a*<sup>-/-</sup> T cells. We tested the hypothesis that IL-22 might mediate the exacerbated wasting disease observed in recipients of *Il17a*<sup>-/-</sup> T cells by using T cells deficient in both IL-17 and IL-22 in additional transfer experiments and found IL-22 was in fact not responsible for the accelerated IBD.

The precise underlying mechanisms driving the wasting disease in this model, in general, remain unidentified so far. As IL-17R is expressed nearly ubiquitously<sup>28</sup>, it remains possible that IL-17 may influence nearly every cell type present in the gut microenvironment. Indeed, IL-17 may positively affect epithelial cell survival or otherwise aid in maintaining the integrity of the epithelial barrier; however, our data suggest that IL-17 may exert its suppressive effect in this model at least in part by suppressing T<sub>H</sub>1 differentiation. Our results suggest that this is probably mediated through the suppression of the induction of T-bet, the 'master regulator' of T<sub>H</sub>1 differentiation. It is important to note that the IL-17-mediated suppression of T-bet expression in our studies was not absolute and was eventually overcome by the T<sub>H</sub>1 differentiation program. As T<sub>H</sub>1-associated cytokines, including IFN- $\gamma$ , potentially inhibit IL-17 expression<sup>29,30</sup>, it is plausible that, physiologically, IL-17 must repress early T<sub>H</sub>1 differentiation to fulfill its critical function in promoting the recruitment of neutrophils to sites of inflammation. Of course, during late-stage chronic disease, persistent IL-17 expression may

also participate in ongoing tissue damage through the recruitment of neutrophils or through other mechanisms. Indeed, we found that IL-17 induced the expression of certain target genes, including the gene encoding the chemokine receptor CCR6, in mature T<sub>H</sub>1 effector cells *in vitro* (W.O., unpublished observations).

In the studies presented here, we have demonstrated the following: IL-17 was not required for cellular infiltration and inflammation of colon tissue in this experimental system; the transferred T cells were responsive to IL-17 *in vivo*, as shown by the wasting disease that resulted from the absence of IL-17R in T cells; despite similar cellular infiltration in the recipient colon tissues at the onset of weight loss, the severity of wasting disease was regulated by IL-17; and the absence of IL-17A or IL-17R in T cells led to an accelerated and severe wasting disease accompanied by higher expression of genes encoding T<sub>H</sub>1-type cytokines. The proinflammatory nature of IL-17, in the context of the environment-specific anti-inflammatory effects of IL-17 we have reported, raises several questions. Is IL-17 (or are IL-17-producing cells) by default proinflammatory and simply held 'at bay' in the gut microenvironment by IL-10 and/or other immunoregulatory factors? Alternatively, perhaps a signaling mechanism exists, a biological 'switch' of sorts that controls many factors in the IL-17-producing cells themselves or in the stromal compartment in mediating the 'pathogenicity' of IL-17-producing cells.

Our data, although paradoxically at odds with some of the literature describing proinflammatory functions for IL-17, are consistent with the idea of a pleiotropic, environment-specific protective function for IL-17 in the gut. Intraepithelial  $\gamma\delta$  T cells protect the intestinal mucosa during chemically induced epithelial damage and aid in maintaining intestinal homeostasis by inhibiting exacerbated inflammatory responses to both foreign antigens and autoantigens<sup>31</sup>. Notably, at steady state,  $\gamma\delta$  T cells are the main IL-17-producing lymphocyte subset in mice<sup>32</sup>. Additional studies are needed to determine if in the absence of observable immunopathology, IL-17 expression indeed aids in maintaining intestinal homeostasis.

## METHODS

Methods and any associated references are available in the online version of the paper at <http://www.nature.com/natureimmunology/>.

## ONLINE METHODS

### Animals

C57BL/6 mice were from The Jackson Laboratory. *Il17a*<sup>-/-</sup> mice have been described<sup>33</sup>. *Il17ra*<sup>-/-</sup> mice (provided by J.K.K.) have also been described<sup>34</sup>. *Rag1*<sup>-/-</sup> mice were maintained by the Yale University Animal Resource Center according to standard protocol. All studies were approved by the Institutional Animal Care and Use Committee of Yale University.

### Cell purification

Splenocyte samples from 6- to 8-week-old C57BL/6 or *Il17a*<sup>-/-</sup> mice were enriched for CD4<sup>+</sup> cells (L3T4 microbeads; Miltenyi Biotec). CD4<sup>+</sup>CD25<sup>-</sup>CD45RB<sup>hi</sup> cells were purified by high-speed cell sorting on a MoFlo cell sorter (Dako Cytomation) with fluorescein isothiocyanate-conjugated anti-CD45RB (16A), phycoerythrin-conjugated anti-CD25 (PC61) and allophycocyanin-conjugated anti-CD4 (RM4-5; all from BD Pharmingen). Sorted cell purity was always over 97%.

### Adoptive transfer studies

Purified CD45RB<sup>hi</sup> cells from unmanipulated wildtype C57BL/6, *Il17a*<sup>-/-</sup> or *Il17ra*<sup>-/-</sup> mice were injected intraperitoneally into *Rag1*<sup>-/-</sup> recipients ( $4 \times 10^5$  cells per mouse in 200 ml sterile PBS per injection). Recipients were weighed throughout the course of the experiments. Colon tissue was resected from recipient mice at various time points after transfer. Tissue samples stained with hematoxylin and eosin were evaluated by microscopy (images are presented at original magnification). Adjacent tissue was collected for extraction of RNA or protein, used for RT-PCR or immunoblot analysis, respectively.

### Gene expression analysis

Tissue samples were disrupted with a rotor-star homogenizer. RNA was extracted from tissue homogenates or from sorted cells cultured *in vitro* with the RNeasy-Qiashredder purification system (Qiagen). After first-strand synthesis by a standard SuperScript II reverse-transcription protocol (Invitrogen), quantitative real-time PCR was done in 96-well optical plates on the ABI 7500 instrument with gene-specific primers and dual-labeled fluorogenic probes (all from Applied Biosystems). Relative expression was quantified by the change in cycle threshold method (DDC<sub>T</sub>) as follows: (C<sub>T</sub> of target gene expression in test sample – C<sub>T</sub> of target gene in control sample) – (C<sub>T</sub> of reference gene in test sample – C<sub>T</sub> of reference gene in control sample), where control samples were always recipients of wild-type (control) T cells. All results were normalized to Hprt1, quantified in parallel amplification reactions during each PCR and are presented as the 'fold induction' with control samples set to an expression index of 1.

### *In vitro* lymphocyte stimulation

Naive CD4<sup>+</sup> T cells were stimulated with plate-bound anti-CD3 and anti-CD28 (5 µg/ml (2C11) and 1 µg/ml (37.5.1), respectively) in neutral (T<sub>H</sub>0) conditions or polarizing (T<sub>H</sub>1) conditions as follows: T<sub>H</sub>0 cells were developed in the presence of neutralizing anti-IFN-γ (XMG1.2) and anti-IL-4 (11B11) at a final concentration of 10 µg/ml of each. T<sub>H</sub>1 cells were generated with IL-12 (3.5 ng/ml) in the presence of anti-IL-4 (11B11). Where indicated, recombinant mouse IL-17 (eBioscience) was added at the time of initial cell seeding, to the final concentrations presented in figures. In some experiments, cells were restimulated for 16 h with plate-bound anti-CD3 (1 mg/ml) and cytokine production was measured by enzyme-linked immunosorbent assay (BD Pharmingen).

### Immunoprecipitation and immunoblot analysis

Anti-T-bet (4B10; Santa Cruz), anti-actin (I-19; Santa Cruz), anti-STAT1 (Cell Signaling) or antibody to STAT1 phosphorylated at tyrosine 701 (Cell Signaling) was used as according to the manufacturer's instructions. Secondary antibodies were from Santa Cruz. Polyclonal anti-mouse IL-17R (AF448; R&D Systems) was used in immunoprecipitation experiments. T cells were lysed in 1% (vol/vol) NonidetP40 and were incubated overnight at 4 °C with 1.5 µg of the immunoprecipitating antibody. Protein A/G beads were used for antibody capture (Pierce). Peptide N-glycosidase F was from New England Biolabs. Standard detection reagents were used for enhanced chemiluminescence development (Pierce). Images were quantified with ImageJ software (National Institutes of Health).

### Lymphocyte proliferation

Naive CD4<sup>+</sup> T cells were purified, stimulated and polarized to T<sub>H</sub>1-type effector cells *in vitro* for 4 d as described above. Cells were cultured in 96-well plates and were pulsed with 1 µCi [<sup>3</sup>H]thymidine on day 3 for a total pulse of 16 h. Wells were collected on day 4 and proliferation was quantified according to a standard protocol.

## Histopathology and semiquantitative tissue analysis

Colons were excised at the ileoceccocolic junction and rectum, were placed in Bouin's fixative solution (Rocca Chemical) for processing and were embedding lengthwise in paraffin (Blue RiBbon; Surgipath Medical Industries). Blocks were sectioned to the level of the lumen and then were serially sectioned (5  $\mu$ m). The first and twentieth sections (of 54 total) were stained with hematoxylin and eosin, followed by placement of coverslips by routine methods. Colons were evaluated and were assigned scores by investigators 'blinded' to experimental manipulation. Each section was evaluated for pathological changes in the mucosa, submucosa, muscularis externa and serosa, including inflammation (location and extent), edema, mucosal changes of ulceration, hyperplasia and attenuation, with crypt loss or abscess noted by examination of hematoxylin and eosin-stained slides assessed at low power and higher power and assigned scores for the presence and extent (severity) of the tissue changes by a semiquantitative criterion-based method adapted from a published method<sup>35</sup>. Severity scores ranged from 0 to 5 as follows: 0, within normal limits or absent; 1, minimal; 2, mild; 3, moderate; 4, marked; and 5, severe. Furthermore, overall thickness of the colon wall was estimated all mice in relation to the internal arrowhead pointer in the microscope (about 95  $\mu$ m at 10 $\times$  magnification; Nikon Instruments) and a subset was measured from digital images. Digital light microscopic images were recorded with a Leica DM550B microscope (Bannockburn), AxioCam MRC camera and AxioVision 4.4 imaging software (Carl Zeiss Microimaging) and were optimized by Adobe Photoshop 8.0. Organ thickness in a subset of colons was evaluated (total thickness, mucosa, submucosa-muscularis externa) with AxioVision 4.4 imaging software (Carl Zeiss Microimaging).

## Statistical analyses

Means and s.d. were calculated according to standard practice. A hierarchical analysis strategy was used for time-dependent weight-loss data in which the first analysis was a repeated-measures ANOVA to assess the significance of the main effects and an experimental group-time interaction. Where the interactive term was significant, post-hoc testing was done with Student's t-test for independent samples, and appropriate P values are reported based on adjustment according to Levene's test for equality of the variance. The  $\alpha$ -levels were set at 0.05 and the Statistical Package for the Social Sciences, release 15.0 was used for all analyses.

## Supplementary Material

Refer to Web version on PubMed Central for supplementary material.

## ACKNOWLEDGMENTS

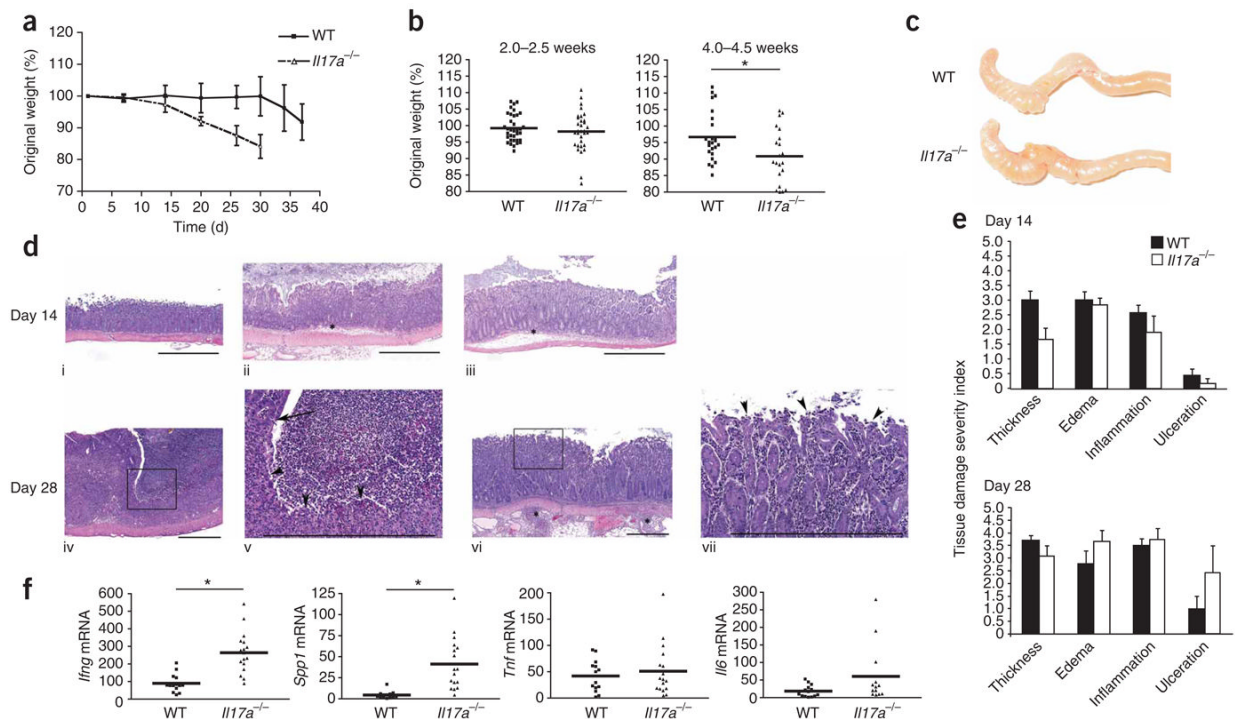
We thank G. Tokmouline for assistance with flow cytometry cell sorting; E. Esplugues for critical reading of the manuscript and comments; A. Lin for assistance with statistical analyses; and F. Manzo for administrative assistance. Supported by the National Multiple Sclerosis Society (W.O.) and the Howard Hughes Medical Institute (R.A.F.).

## References

1. Langrish CL, et al. IL-12 and IL-23: master regulators of innate and adaptive immunity. *Immunol. Rev* 2004;202:96–105. [PubMed: 15546388]
2. Aggarwal S, Ghilardi N, Xie MH, de Sauvage FJ, Gurney AL. Interleukin-23 promotes a distinct CD4 T cell activation state characterized by the production of interleukin-17. *J. Biol. Chem* 2003;278:1910–1914. [PubMed: 12417590]
3. Kastelein RA, Hunter CA, Cua DJ. Discovery and biology of IL-23 and IL-27: related but functionally distinct regulators of inflammation. *Annu. Rev. Immunol* 2007;25:221–242. [PubMed: 17291186]
4. Oppmann B, et al. Novel p19 protein engages IL-12p40 to form a cytokine, IL-23, with biological activities similar as well as distinct from IL-12. *Immunity* 2000;13:715–725. [PubMed: 11114383]

5. Cua DJ, et al. Interleukin-23 rather than interleukin-12 is the critical cytokine for autoimmune inflammation of the brain. *Nature* 2003;421:744–748. [PubMed: 12610626]
6. Langrish CL, et al. IL-23 drives a pathogenic T cell population that induces autoimmune inflammation. *J. Exp. Med* 2005;201:233–240. [PubMed: 15657292]
7. Honorati MC, et al. High in vivo expression of interleukin-17 receptor in synovial endothelial cells and chondrocytes from arthritis patients. *Rheumatology (Oxford)* 2001;40:522–527. [PubMed: 11371660]
8. Fossiez F, et al. T cell interleukin-17 induces stromal cells to produce proinflammatory and hematopoietic cytokines. *J. Exp. Med* 1996;183:2593–2603. [PubMed: 8676080]
9. Schwarzenberger P, et al. IL-17 stimulates granulopoiesis in mice: use of an alternate, novel gene therapy-derived method for in vivo evaluation of cytokines. *J. Immunol* 1998;161:6383–6389. [PubMed: 9834129]
10. Laan M, et al. Neutrophil recruitment by human IL-17 via C-X-C chemokine release in the airways. *J. Immunol* 1999;162:2347–2352. [PubMed: 9973514]
11. Duerr RH, et al. A genome-wide association study identifies IL23R as an inflammatory bowel disease gene. *Science* 2006;314:1461–1463. [PubMed: 17068223]
12. Dubinsky MC, et al. IL-23 receptor (IL-23R) gene protects against pediatric Crohn's disease. *Inflamm. Bowel Dis* 2007;13:511–515. [PubMed: 17309073]
13. Breese E, Braegger CP, Corrigan CJ, Walker-Smith JA, MacDonald TT. Interleukin-2- and interferon- $\gamma$ -secreting T cells in normal and diseased human intestinal mucosa. *Immunology* 1993;78:127–131. [PubMed: 8436398]
14. Fujino S, et al. Increased expression of interleukin 17 in inflammatory bowel disease. *Gut* 2003;52:65–70. [PubMed: 12477762]
15. Kullberg MC, et al. IL-23 plays a key role in *Helicobacter hepaticus*-induced T cell-dependent colitis. *J. Exp. Med* 2006;203:2485–2494. [PubMed: 17030948]
16. Yen D, et al. IL-23 is essential for T cell-mediated colitis and promotes inflammation via IL-17 and IL-6. *J. Clin. Invest* 2006;116:1310–1316. [PubMed: 16670770]
17. Hue S, et al. Interleukin-23 drives innate and T cell-mediated intestinal inflammation. *J. Exp. Med* 2006;203:2473–2483. [PubMed: 17030949]
18. Powrie F, et al. Inhibition of Th1 responses prevents inflammatory bowel disease in scid mice reconstituted with CD45RB<sup>hi</sup> CD4<sup>+</sup> T cells. *Immunity* 1994;1:553–562. [PubMed: 7600284]
19. Ito H, Fathman CG. CD45RB<sup>high</sup> CD4<sup>+</sup> T cells from IFN- $\gamma$  knockout mice do not induce wasting disease. *J. Autoimmun* 1997;10:455–459. [PubMed: 9376073]
20. Zhang Z. Critical role of IL-17 receptor signaling in acute TNBS-induced colitis. *Inflamm. Bowel Dis* 2006;12:382–388. [PubMed: 16670527]
21. Ogawa A. Neutralization of interleukin-17 aggravates dextran sulfate sodium-induced colitis in mice. *Clin. Immunol* 2004;110:55–62. [PubMed: 14962796]
22. Tlaskalová-Hogenová H. Involvement of innate immunity in the development of inflammatory and autoimmune diseases. *Ann. NY Acad. Sci* 2005;1051:787–798. [PubMed: 16127016]
23. O'Regan AW, Hayden JM, Berman JS. Osteopontin augments CD3-mediated interferon-gamma and CD40 ligand expression by T cells, which results in IL-12 production from peripheral blood mononuclear cells. *J. Leukoc. Biol* 2000;68:495–502. [PubMed: 11037970]
24. Renkl AC, et al. Osteopontin functionally activates dendritic cells and induces their differentiation toward a Th1-polarizing phenotype. *Blood* 2005;106:946–955. [PubMed: 15855273]
25. Chen Z, et al. Selective regulatory function of Socs3 in the formation of IL-17-secreting T cells. *Proc. Natl. Acad. Sci. USA* 2006;103:8137–8142. [PubMed: 16698929]
26. Yang XO, et al. Regulation of inflammatory responses by IL-17F. *J. Exp. Med* 2008;205:1063–1075. [PubMed: 18411338]
27. Zheng Y, et al. Interleukin-22, a Th17 cytokine, mediates IL-23-induced dermal inflammation and acanthosis. *Nature* 2007;445:648–651. [PubMed: 17187052]
28. Kolls JK, Linden A. Interleukin-17 family members and inflammation. *Immunity* 2004;21:467–476. [PubMed: 15485625]

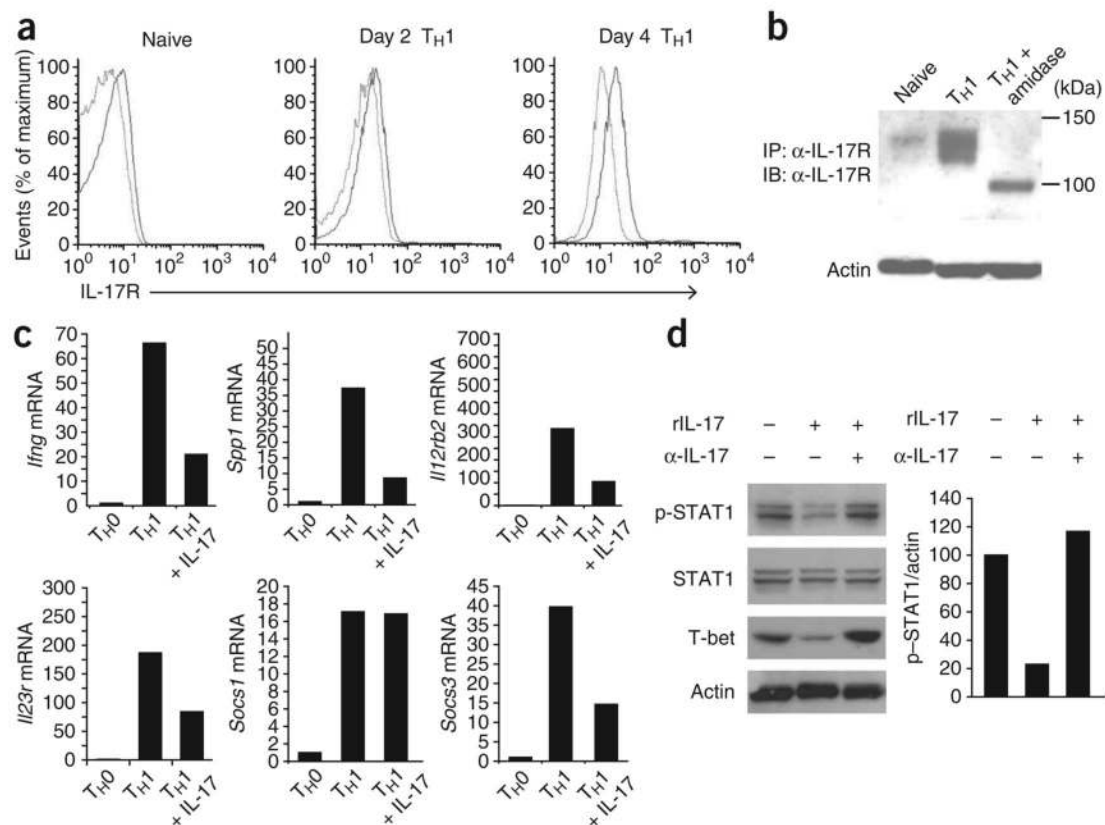
29. Park H, et al. A distinct lineage of CD4 T cells regulates tissue inflammation by producing interleukin 17. *Nat. Immunol* 2005;6:1133–1141. [PubMed: 16200068]
30. Harrington LE. Interleukin 17-producing CD4<sup>+</sup> effector T cells develop via a lineage distinct from the T helper type 1 and 2 lineages. *Nat. Immunol* 2005;6:1123–1132. [PubMed: 16200070]
31. Boismenu R, Chen Y, Havran WL. The role of intraepithelial gammadelta T cells: a gut-feeling. *Microbes Infect* 1999;1:235–240. [PubMed: 10801235]
32. Stark MA, et al. Phagocytosis of apoptotic neutrophils regulates granulopoiesis via IL-23 and IL-17. *Immunity* 2005;22:285–294. [PubMed: 15780986]
33. Nakae S, et al. Antigen-specific T cell sensitization is impaired in IL-17-deficient mice, causing suppression of allergic cellular and humoral responses. *Immunity* 2002;17:375–387. [PubMed: 12354389]
34. Ye P, et al. Requirement of interleukin 17 receptor signaling for lung CXC chemokine and granulocyte colony-stimulating factor expression, neutrophil recruitment, and host defense. *J. Exp. Med* 2001;194:519–527. [PubMed: 11514607]
35. Montgomery RR, et al. Recruitment of macrophages and polymorphonuclear leukocytes in Lyme carditis. *Infect. Immun* 2007;75:613–620. [PubMed: 17101663]



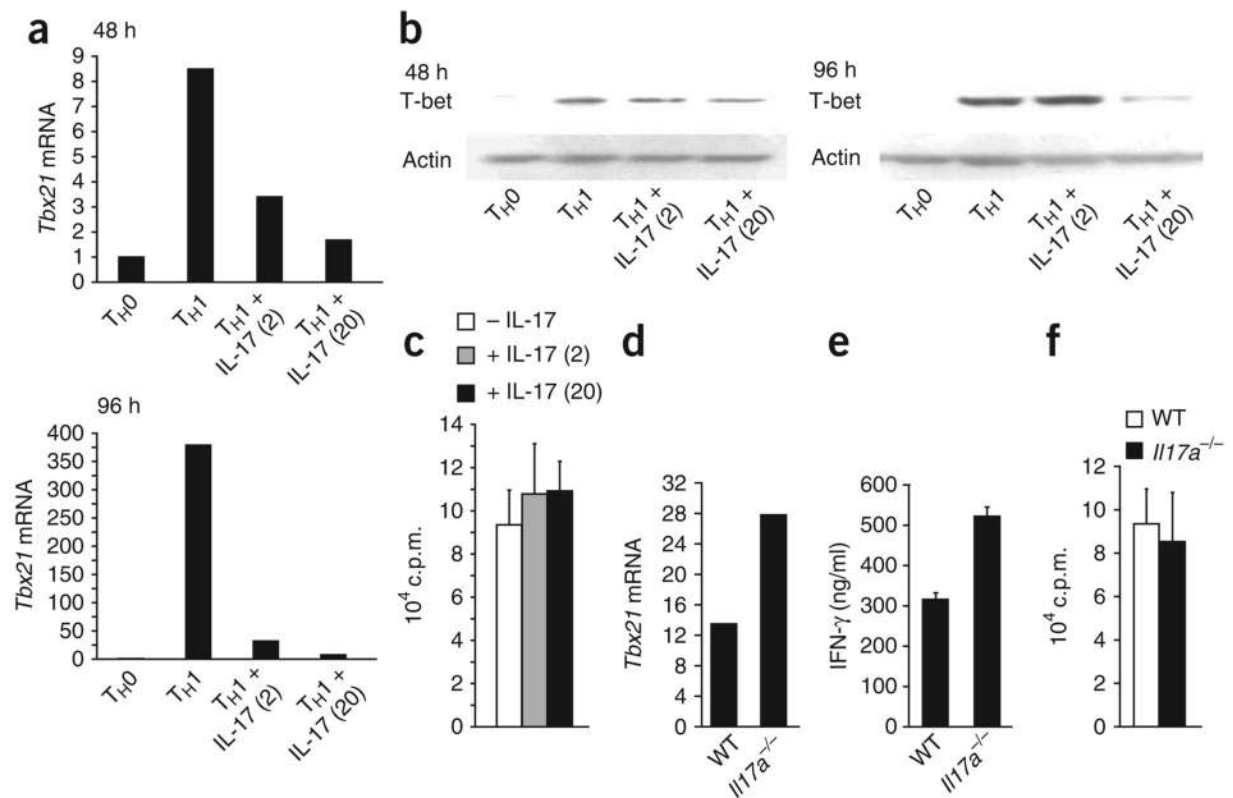
**Figure 1.**

IL-17A-deficient CD45RB<sup>hi</sup> T cells induce an aggressive wasting disease in *Rag1*<sup>-/-</sup> recipient mice. **(a)** Body weights of *Rag1*<sup>-/-</sup> recipients of intraperitoneally injected purified CD45RB<sup>hi</sup> CD4<sup>+</sup> T cells from *Il17a*<sup>-/-</sup> mice or unmanipulated wild-type (WT) C57BL/6 mice on day 0, presented as percent of original weight. Data are group averages from one experiment (error bars, s.e.m.). **(b)** Weight loss distributions of each individual mouse (single symbols) and composite statistics of all recipient mice. Means (small horizontal bars) at day 14 ( $P = 0.4155$ ): recipients of wild-type cells ( $n = 35$ ), 99.26 (s.d., 4.168); recipients of *Il17a*<sup>-/-</sup> cells ( $n = 32$ ), 99.22 (s.d., 6.057). Means at day 28: recipients of wild-type cells ( $n = 24$ ), 96.71 (s.d., 7.493); recipients of *Il17a*<sup>-/-</sup> cells ( $n = 21$ ), 90.87 (s.d., 8.155). \*,  $P \leq 0.01$ . Data are representative of three independent experiments. **(c)** Gross organ morphology of the cecum and ascending colon from the recipient mice in **b** at day 28. Results are representative of three experiments. **(d)** Histology of colon tissues from the mice in **a**. Top, colon tissues at day 14 from an unmanipulated wild-type mouse (i), a recipient of *Il17a*<sup>-/-</sup> cells (ii) or a recipient of wild-type cells (iii). \*, edema. Bottom, colon tissues at day 28 from a recipient of *Il17a*<sup>-/-</sup> cells (iv and v (higher magnification of box in iv)), or wild-type cells (vi and vii (higher magnification of box in vi)). Arrowheads indicate the presence (iv,v) or absence (vi,vii) of ulcerated epithelium. Scale bars, 500  $\mu$ m. Results are representative of two experiments. **(e)** Quantification of pathological changes in the mice in **a**, assessed as 'severity scores'. Data are representative of two experiments (error bars, s.e.m.). **(f)** Quantitative RT-PCR analysis of mRNA transcripts encoding cytokines (vertical axes), measured in ascending colon tissue from the mice in **a** on day 28. Each dot represents an individual mouse; scores are presented as 'fold increase' relative to baseline expression in colon tissue from unmanipulated wild-type littermates after normalization to expression of *Hprt1* (encoding hypoxanthine guanine phosphoribosyl transferase; change in cycling threshold method). Means for *Ifng* ( $P \leq 0.0001$ ): recipients of wild-type cells ( $n = 14$ ), 89.79; recipients of *Il17a*<sup>-/-</sup> cells ( $n = 17$ ), 263.8. Means for *Spp1* ( $P \leq 0.001$ ): recipients of wild-type cells ( $n = 13$ ), 4.56; recipients of *Il17a*<sup>-/-</sup> cells ( $n = 17$ ), 41.25. Means for *Il6*: recipients of wild-type cells ( $n = 14$ ), 60.48; recipients of

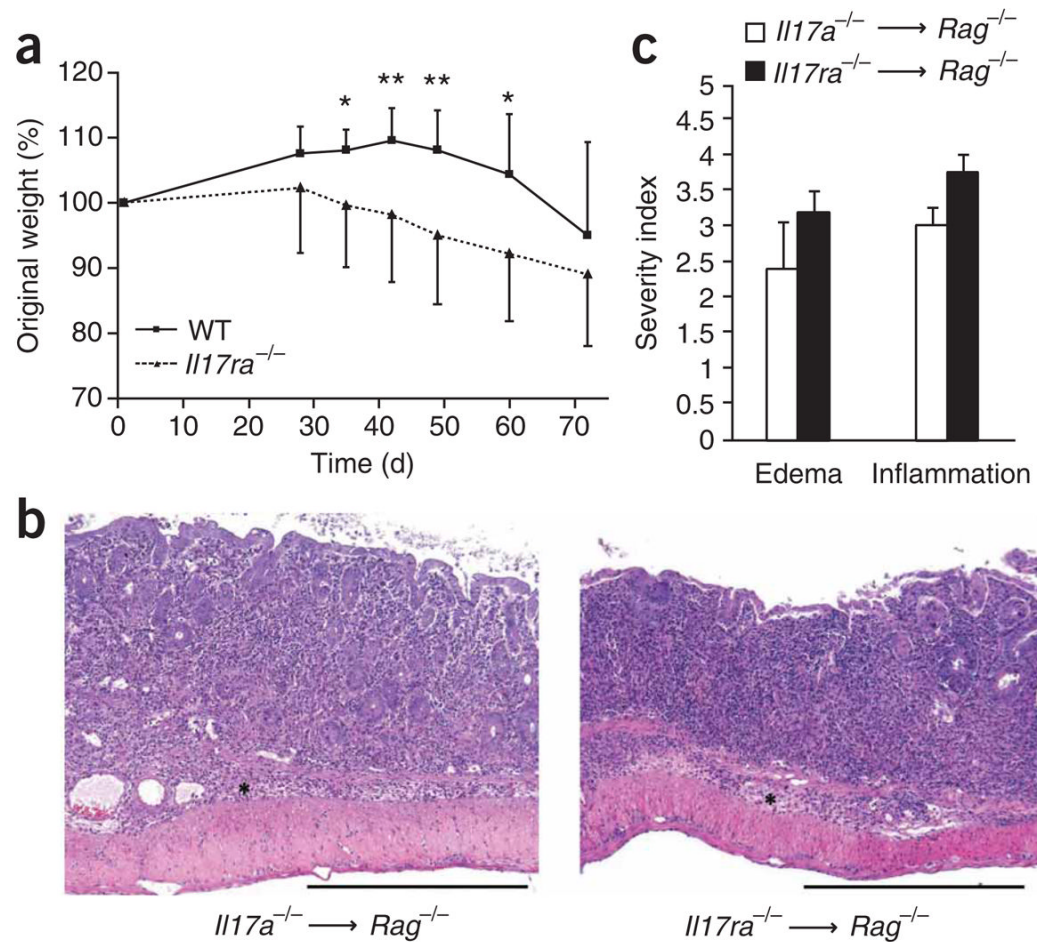
*Il17ra*<sup>-/-</sup> T cells ( $n = 13$ ), 18.62. \*,  $P \leq 0.001$  (unpaired, two-tailed Student's *t*-test). Data are representative of three experiments.

**Figure 2.**

IL-17 modulates T<sub>H</sub>1 differentiation. **(a)** Flow cytometry analysis of IL-17R on the cell surface of naive CD4<sup>+</sup> T cells assessed directly after isolation (Naive) or after 2 d or 4 d of culture in T<sub>H</sub>1-polarizing conditions. Light lines, isotype-matched control antibody; dark lines, antibody to IL-17R. Data are representative of two experiments. **(b)** Immunoblot analysis (IB) of the immunoprecipitation (IP) of IL-17R from freshly isolated naive CD4<sup>+</sup> T cells or from T cells cultured for 4 d in T<sub>H</sub>1-polarizing conditions *in vitro* with (right) or without (left and middle) amidase treatment. Actin, loading control for protein content in cell lysates. α-IL-17R, antibody to IL-17R. Results are representative of two independent experiments. **(c)** Real-time PCR analysis of gene expression in T<sub>H</sub>0 effector cells or in T<sub>H</sub>1 effector cells at day 4 generated *in vitro* in the presence (+ IL-17) or absence of recombinant IL-17 (20 ng/ml). Data are representative of three experiments. **(d)** Immunoblot analysis (left) of T<sub>H</sub>1 effector cells at day 4 generated *in vitro* in the presence (+) or absence (–) of recombinant IL-17 (rIL-17) and/or IL-17-neutralizing antibody (α-IL-17). Right, differences in expression of phosphorylated STAT1 (p-STAT1), normalized to actin and presented relative to that of day-4 T<sub>H</sub>1 cells cultured alone. Data are representative of three experiments.

**Figure 3.**

IL-17 suppresses the induction of T-bet in maturing T<sub>H</sub>1 cells. **(a)** Real-time PCR analysis of *Tbx21* in T<sub>H</sub>0 effector cells or in T<sub>H</sub>1 effector cells polarized *in vitro* in the presence (+ IL-17) or absence of 2 ng/ml or 20 ng/ml (in parentheses) of recombinant mouse IL-17 after 48 h or 96 h of culture, normalized to *Hprt1* expression and presented as 'fold increase' relative to that of T<sub>H</sub>0 cells. **(b)** Immunoblot analysis of T-bet in the 96-hour cultures in **a**. Actin, loading control. Data are representative of three or more independent experiments (**a,b**). **(c)** Proliferation of cells in T<sub>H</sub>1 effector cultures at day 4, differentiated in the presence or absence of 2 ng/ml or 20 ng/ml (in parentheses) of recombinant mouse IL-17, assessed by incorporation of [<sup>3</sup>H]thymidine. Data are representative of two independent experiments. **(d)** *Tbx21* expression in day-4 T<sub>H</sub>1 effector cells generated *in vitro* from wild-type or *Il17a*<sup>-/-</sup> naive CD4<sup>+</sup> CD45RB<sup>hi</sup> T cells, normalized to *Hprt1* expression and presented as 'fold increase' relative to that of T<sub>H</sub>0 cells. Data are representative of three experiments. **(e)** Enzyme-linked immunosorbent assay of the release of IFN-γ from naive wild-type or *Il17a*<sup>-/-</sup> CD4<sup>+</sup> CD45RB<sup>hi</sup> T cells polarized for 5 d in T<sub>H</sub>1-type conditions before overnight restimulation. Data are representative of three experiments. **(f)** Proliferation of the cells in **d**, assessed by incorporation of [<sup>3</sup>H]thymidine. Data are representative of three experiments.

**Figure 4.**

*Il17ra*<sup>-/-</sup> CD45RB<sup>hi</sup> donor T cells elicit an accelerated wasting disease in *Rag1*<sup>-/-</sup> recipients.

(a) Composite weight-loss curves of recipients of adoptive transfer of wild-type or *Il17ra*<sup>-/-</sup> CD45RB<sup>hi</sup> CD4<sup>+</sup> T cells (number of mice with weight loss, Table 1).  $P \leq 0.01$ , time;  $P \leq 0.01$ , experimental group;  $P \leq 0.01$ , time-group interaction (repeated-measures ANOVA). \*,  $P < 0.05$ , \*\*,  $P \leq 0.01$ , days 35–60 after transfer of cells (post-hoc *t*-test); means at day 35: recipients of wild-type T cells ( $n = 8$ ), 108.1; recipients of *Il17ra*<sup>-/-</sup> T cells ( $n = 8$ ), 99.59. Data are representative of two independent experiments with similar results (error bars, s.d.). (b) Hematoxylin and eosin–stained sections of *Rag1*<sup>-/-</sup> recipient colons obtained at day 28 after adoptive transfer *Il17a*<sup>-/-</sup> or *Il17ra*<sup>-/-</sup> T cells. Scale bars, 500  $\mu$ m. Results are representative of two experiments. (c) Histological quantification of edema and inflammation in colons from *Rag1*<sup>-/-</sup> recipient mice, obtained at day 28 after adoptive transfer of *Il17a*<sup>-/-</sup> or *Il17ra*<sup>-/-</sup> T cells, presented as ‘severity scores’. There were no statistically significant differences among the groups for any criteria. Data are representative of two experiments (error bars, s.e.m.).

**Table 1**  
Accelerated disease course in *Rag1*<sup>-/-</sup> recipients of *Il17ra*<sup>-/-</sup> T cells

	Day 35	Day 42	Day 49	Day 60	Day 72
Recipients of WT T cells	0/9	0/9	0/9	3/9	6/9
Recipients of <i>Il17ra</i> <sup>-/-</sup> T cells	3/8	4/8	5/8	6/8	6/8

Disease incidence (mass loss) in recipients of wild-type or *Il17ra*<sup>-/-</sup> T cells at five time points, presented as mice with disease/total mice in group. Data are from one experiment representative of two independent experiments with similar results.